Iranian Journal of Chemical Engineering

Journal Homepage: www.ijche.com

pISSN: 1735-5397
eISSN: 2008-2355

Elimination of Heavy Metal Contaminants from Wastewater through the Nanoparticle-Assisted Treatment under Ultrasonic Waves

Faezeh Mohammadi

Department of Chemical Engineering, Ker. C., Islamic Azad University, Kermanshah, Iran

ARTICLE INFO

Article type:
Research article

Article history:
Received: 2026-01-16
Revised: 2026-02-04
Accepted: 2026-02-20
Available online: 2026-02-22

Keywords:
Ultrasonic irradiation,
Fe_3O_4 nanoparticles,
Nickel (II) removal,
Adsorption,
Wastewater treatment

ABSTRACT

Heavy metals are among the most hazardous pollutants released into the environment through industrial activities. In recent years, adsorption has been recognized as an effective method for the removal of metal ions from wastewater. Ultrasonic irradiation is a promising technique for intensifying mass transfer during adsorption. In this study, the effect of high-frequency ultrasonic waves on the enhancement of the removal of nickel (II) ion from aqueous solutions using Fe_3O_4 nanoparticles was investigated. The influence of the dosage of adsorbenst, contact time, and pH on the removal efficiency was examined to optimize the removal efficiency using the response surface methodology (RSM). The maximum removal efficiency, achieved with the ultrasound-assisted process, was 84.3% at the contact time of 60 minutes, 8 g of Fe_3O_4, and pH = 5, while the conventional stirring (shaker) method resulted in a maximum efficiency of 79.54% at 100 minutes, 10 g of adsorbent, and pH = 9. The use of ultrasound significantly accelerated the adsorption rate at the initial stages by generating cavitation and microstreaming, which increased the availability of active surface sites on the nanoparticles. These findings demonstrate that the combination of Fe_3O_4 nanoparticles and ultrasonic irradiation offers a rapid, efficient, and environmentally friendly approach for the removal of nickel (II) ions from industrial wastewater.

DOI: 10.22034/ijche.2026.547502.1574 URL: https://www.ijche.com/article_241005.html

1. Introduction

Heavy metal pollution has become one of the most serious environmental concerns due to rapid industrialization and urban development. Metals such as nickel (Ni), cadmium (Cd), lead (Pb), and chromium (Cr) are toxic even at low concentrations and tend to bioaccumulate through the food chain, posing severe risks to

*Corresponding author: Faezehmohammadi@iau.ac.ir

ecosystems and human health [1–4]. Their persistence and non-biodegradability make their removal from industrial effluents particularly challenging. Many conventional remediation techniques, such as chemical precipitation, ion-exchange systems, membrane-based separations, and various electrochemical approaches, suffer from drawbacks including substantial operating expenses, incomplete contaminant elimination, and the formation of additional secondary wastes [5,6]. Therefore, adsorption has emerged as one of the most effective, economical, and environmentally friendly techniques for removing heavy metal from aqueous systems [7,8].

Nanotechnology has recently opened up new opportunities to improve the efficiency of adsorption-based wastewater treatment. Among various nanomaterials, magnetic iron oxide nanoparticles (Fe_3O_4) have attracted remarkable attention owing to their large specific surface area, magnetic separability, biocompatibility, and ability to be reused without significant loss of performance [9,10]. These nanoparticles provide numerous active adsorption sites and can be easily recovered by applying an external magnetic field, which enhances both process efficiency and sustainability. Moreover, the surface modification of Fe_3O_4 nanoparticles with organic or inorganic ligands further increases their affinity toward metal ions, leading to improved the adsorption performance [11-13].

At the same time, ultrasonic irradiation has been recognized as an effective intensification technique in water and wastewater treatment. Ultrasound generates cavitation, microstreaming, and localized turbulence that enhance mass transfer and accelerate surface reactions [14,15]. The collapse of cavitation bubbles produces transient high temperatures and pressures, which help disperse nanoparticles, prevent their agglomeration, and expose more active sites for adsorption [16-18]. It has been reported in several studies that the combination of ultrasound and nanomaterials improves adsorption kinetics and increases the efficiency of heavy metal removal compared to conventional stirring methods [19-23].

The integration of ultrasonic irradiation with magnetic nanoparticle-based adsorption thus represents a promising hybrid approach for sustainable wastewater purification. However, despite numerous studies conducted on nanoparticle synthesis and ultrasonic chemistry, few investigations have systematically evaluated the combined effect of ultrasound and Fe_3O_4 nanoparticles for heavy metal removal. In particular, there is still limited understanding of the interplay of pH, contact time, and adsorbent dosage under ultrasonic conditions. Therefore, it is aimed in the present study to investigate the effect of high-frequency ultrasonic waves on the adsorption of nickel (II) ions from aqueous solutions using Fe_3O_4 nanoparticles. The Response Surface Methodology (RSM) was employed to optimize the operating parameters and analyze their interactions. The findings provide insight into the potential of the ultrasound-assisted adsorption as a rapid, efficient, and environmentally sustainable process for industrial wastewater treatment.

2. Materials and methods

2.1. Materials

All chemicals used in this study were of analytical grade. Nickel nitrate hexahydrate ($Ni(NO_3)_2 \cdot 6H_2O$, ≥99% purity) was obtained from Merck (Germany) and used as the source of Ni(II) ions. Iron oxide (Fe_3O_4) nanoparticles were supplied by Asia Research Company (Iran) with an average particle size of 20–30 nm and a specific surface area of approximately 75 m^2/g. Sodium hydroxide (NaOH, 0.1 M) and hydrochloric acid (HCl,

0.1 M) were used to adjust the pH. All aqueous solutions were prepared with double-distilled water (Lab Tech GS-1330, Korea).

The initial nickel stock solution (100 mg/L) was prepared by dissolving 0.100 g of $Ni(NO_3)_2 \cdot 6H_2O$ in 1 L of distilled water. Test solutions with different concentrations were obtained by appropriate dilution. The pH of the solutions was measured using a digital pH meter (Eutech pH 700, Singapore).

2.2. Experimental setup

A custom-designed glass reactor was constructed to evaluate the effect of ultrasonic irradiation. The reactor, with internal dimensions of 30 cm × 15 cm × 12 cm and equipped with five piezoelectric transducers (frequency 1.7 MHz, diameter 2.5 cm), was fixed to the bottom surface through watertight rubber gaskets. The arrangement ensured uniform sound propagation throughout the liquid volume. Each transducer could be individually activated through an external control unit.

To prevent vibration leakage and ensure consistent energy transmission, each transducer was mounted using plastic glands and rubber washers. The overall setup was designed to allow direct contact between the ultrasonic source and the fluid, resulting in effective energy transfer and enhanced cavitation generation. A schematic diagram of the ultrasonic reactor and transducer arrangement is illustrated in Figure 1.

For comparison, a mechanical shaker (IKA KS 130 basic, Germany) operating at 150 rpm was used under identical conditions without ultrasonic assistance.

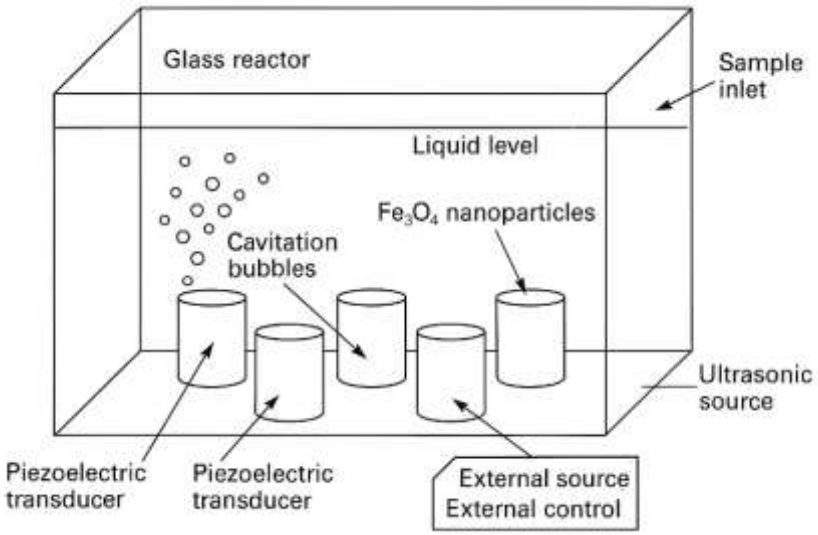

Figure 1. Schematic diagram of the ultrasonic reactor used for Ni(II) removal experiments.

2.3. Experimental procedure

In each experiment, a known mass of Fe_3O_4 nanoparticles (2–10 g) was added to 500 mL of Ni(II) solution with the initial concentration of 100 mg/L. The effects of three independent parameters—the pH (1–9), contact time (20–100 min), and adsorbent dosage (2–10 g)—on the removal efficiency were studied according to a Central Composite Design (CCD) under the Response Surface Methodology (RSM) framework. All experiments were performed at room temperature (25 ± 2 °C). After the adsorption process, samples were separated from the suspension using an external magnet. The concentration of the residual Ni(II) was determined spectrophotometrically using a

UV–Vis spectrophotometer (Shimadzu UV-1800, Japan) at 232 nm. The efficiency of Ni(II) removal was calculated using the following equation:

$$R(\%) = \frac{C_0 - C_e}{C_0} \times 100 \quad (1)$$

where C_0 and C_e (mg/L) are the initial and equilibrium concentrations of Ni(II) ions respectively. All measurements were performed in triplicate, and the average values were reported along with corresponding standard deviations.

2.4. Experimental design and statistical analysis

The optimization of process variables and analysis of the interaction were carried out using the Design Expert software (version 11.1, Stat-Ease Inc., USA). A three-factor, five-level Central Composite Design (CCD) was employed, considering the pH (A), contact time (B), and adsorbent dosage (C) as independent variables. The selection of these three variables and their respective ranges was guided by the preliminary investigations summarized in Table 1.

Table 1.
Coded and reviewed levels of experimental variables.

Name	Units	Low	High	-alpha	+alpha
pH	-	1	9	3	7
Contact time	min	20	100	40	80
Adsorbent mass	g	2	10	4	8

The performance and adequacy of the model were assessed using analysis of variance (ANOVA), along with the coefficient of determination (R^2) and adjusted R^2. Statistical significance was evaluated at the 0.05 significance level ($p < 0.05$).

3.Ressults and discussion

3.1. Adequacy of the model

The adequacy of the proposed quadratic model was assessed through the analysis of variance (ANOVA) to determine the statistical significance of each term and the overall fitness of the model. The results of the experimental design matrix and corresponding responses for both systems (ultrasonic and shaker) are summarized in Table 2, while the ANOVA results are presented in Tables 3.

As shown in Table 3, for the ultrasound-assisted removal of Ni(II), the model exhibited a very high F-value of 116.61 and a very low p-value (< 0.0001), confirming the strong significance of the regression model. Similarly, for the shaker system, the obtained F-value (123.46) and p-value (< 0.0001) indicate excellent statistical reliability. These results demonstrate that the selected quadratic models are highly significant and capable of predicting the experimental data with great accuracy.

Table 2.
Experimental ranges of the independent parameters applied to CCD design.

	Factors			Responses	
Run	**A:pH**	**B:Contact time**	**C:Adsorbent mass**	**Removal efficiency-US (Y1)**	**Removal efficiency-SH (Y2)**
	-	min	g	(%)	(%)
1	5	60	4	76.67	70.23
2	9	100	10	62.5	79.54
3	1	20	2	37.4	34.23
4	7	60	6	82.8	78.12
5	5	60	6	80.12	74.35
6	9	20	2	45.8	42.98
7	1	100	10	52.9	71.26
8	5	80	6	72.2	78.34
9	9	100	2	53.23	74.04
10	5	40	6	72.49	60.22
11	5	60	6	82.91	73.03
12	3	60	6	75.17	69.45
13	5	60	6	80.34	73.38
14	1	100	2	41.18	65.59
15	5	60	8	84.3	75.45
16	9	20	10	48.34	43.88
17	1	20	10	43.24	40.45

Table 3.
ANOVA test for the response functions for the efficiencies of nickel removal with ultrasound.

Source	**Sum of Squares**	**df**	**Mean Square**	**F-value**	**p-value**	
Model	4520.89	9	502.32	116.61	< 0.0001	significant
A-pH	178.62	1	178.62	41.46	0.0004	
B-Contact time	143.17	1	143.17	33.24	0.0007	
C-Adsorbent mass	129.56	1	129.56	30.07	0.0009	
AB	8.30	1	8.30	1.93	0.0476	
AC	4.13	1	4.13	0.9594	0.3600	
BC	19.88	1	19.88	4.61	0.0498	
A^2	2.87	1	2.87	0.6658	0.4414	
B^2	173.26	1	173.26	40.22	0.0004	
C^2	0.8052	1	0.8052	0.1869	0.6785	
Residual	30.15	7	4.31			
Lack of Fit	25.34	5	5.07	2.11	0.3525	not significant
Pure Error	4.81	2	2.41			
Cor Total	4551.05	16				

R^2: 0. 0.9934; adjusted R^2: 0.9849

Among the studied parameters, the pH, contact time, and adsorbent mass were identified as the most influential factors ($p < 0.05$). The contact time showed the highest contribution to the model for the shaker system, while under ultrasonic conditions both the pH and contact time significantly affected the removal efficiency.

Figure 2 illustrates the correlation between the predicted and experimental responses for both the ultrasonic and shaker systems. The nearly linear distribution of the data points indicates an excellent agreement between the model predictions and the actual

experimental results. Moreover, the residual plots display a random dispersion of points around the zero line, confirming the homoscedasticity and normal distribution of the residuals, thereby validating the fundamental assumptions of the developed model.

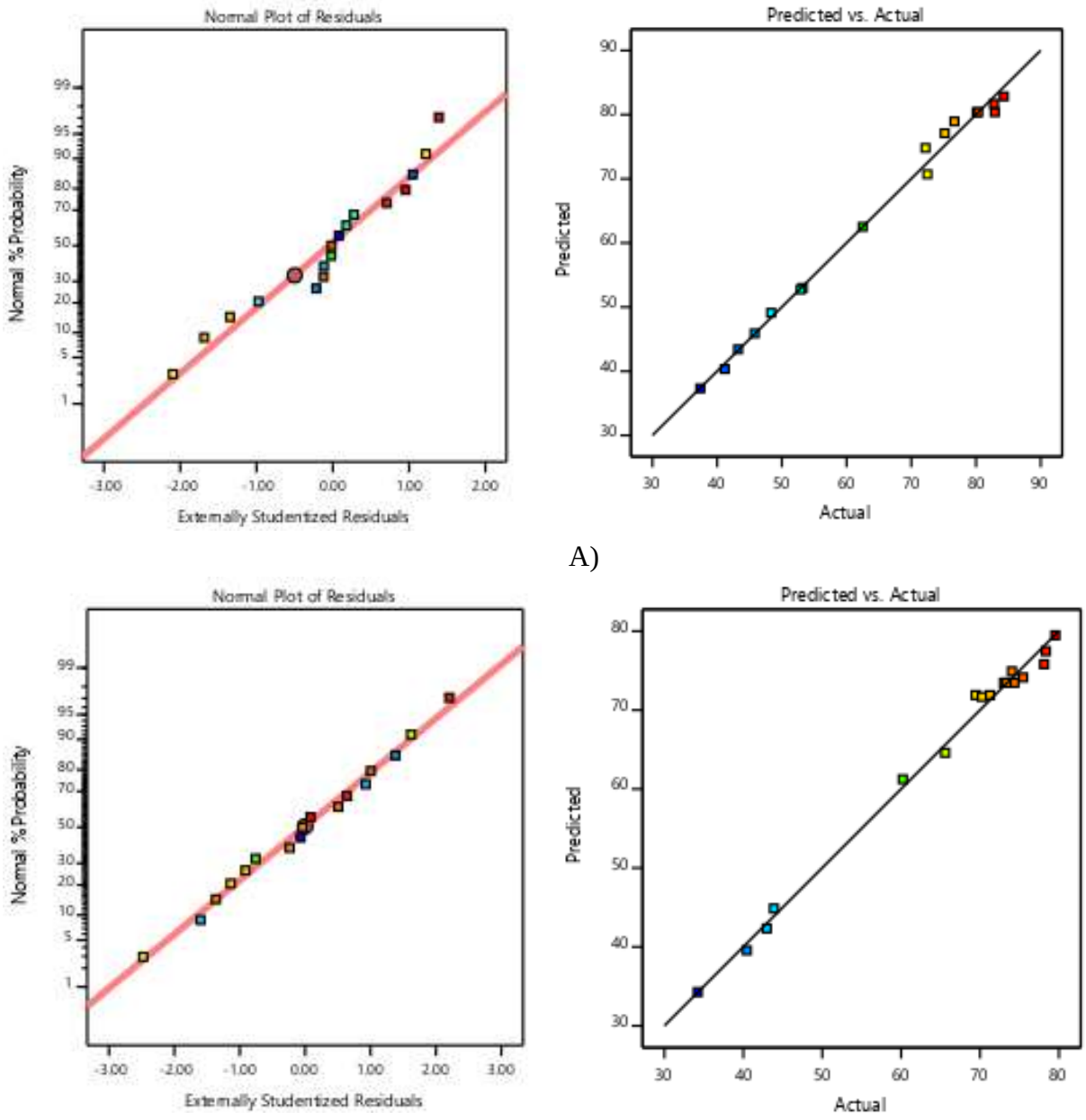

Figure 2. Statistical charts, the normal plot of residuals and the predicted vs. the actual for the (A): ultrasonic system (B): shaker.

Overall, the ANOVA results and diagnostic plots strongly support the adequacy of the developed RSM models for describing and predicting the efficiency of Ni(II) removal under both ultrasonic and shaker conditions.

3.2. Effect of factors on the efficiency of ni(ii) removal

3.2.1. Effect of pH

Figure 3 shows that the efficiency of Ni(II) removal increases by rising the pH value for

both ultrasonic and shaker systems, reaching a maximum under near-neutral to slightly alkaline conditions (pH ≈ 6–9). At low pH values, the protonation of surface hydroxyl groups makes the Fe_3O_4 adsorbent positively charged, causing electrostatic repulsion with Ni^{2+} ions and reducing adsorption. As the pH value increases, deprotonation produces negatively charged sites that facilitate metal ion binding.

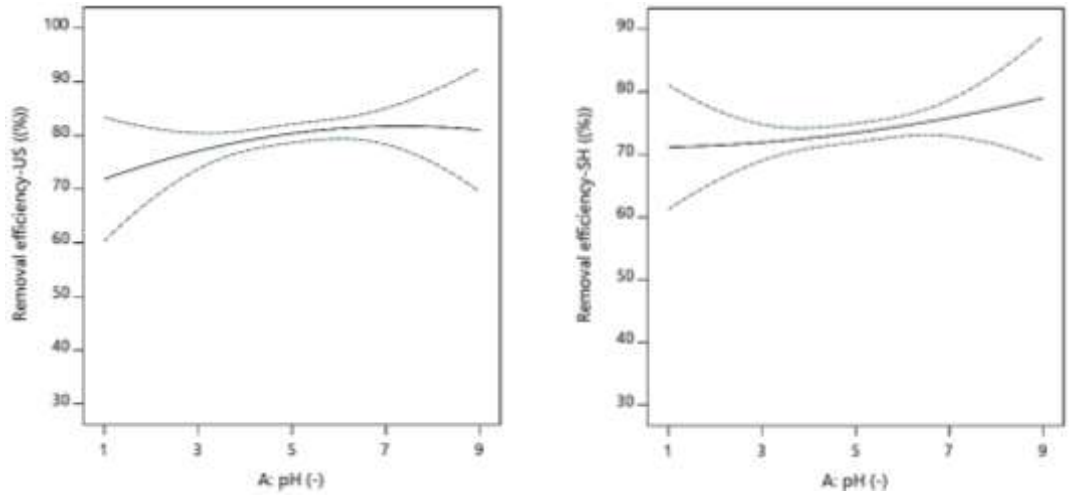

A) **B)**

Figure 3. Effect of the pH on the efficiency of Ni(II) removal, (A): ultrasonic system (B): shaker.

At the pH values of above 8, a slight decline in the removal efficiency may occur due to the formation of $Ni(OH)_2$ precipitates. These results agree with previous reports on Fe_3O_4-based nanomaterials, confirming that pH plays a key role in adsorption behavior and that ultrasonic irradiation significantly enhances performance [7,11,19,20,24].

3.2.2. Effect of the contact time

Figure 4 demonstrates that the efficiency of Ni(II) removal increases with the contact time for both ultrasonic and shaker systems, confirming that adsorption is time-dependent. The initial stage (0–30 min) exhibited rapid uptake due to the large number of the available active sites on Fe_3O_4 nanoparticles and an intense driving force for mass transfer. As adsorption sites became saturated, the rate gradually declined and reached equilibrium. Under ultrasonic irradiation, equilibrium was achieved within about 60 min with the maximum removal efficiency of 84.3 %, while the shaker system required 80–100 min to reach a comparable value (≈79.5 %). The faster kinetics in the ultrasonic system are attributed to acoustic cavitation, which enhances micro-mixing, disrupts boundary layers, and accelerates ion diffusion between phases.

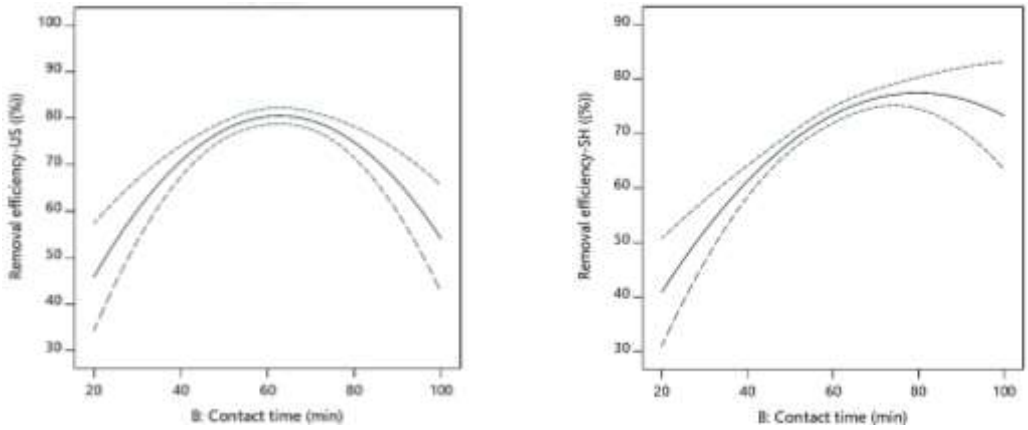

A) **B)**

Figure 4. Effect of the contact time on the efficiency of Ni(II) removal, (A): ultrasonic system (B): shaker.

In contrast, in the shaker system, the process is governed primarily by the external film diffusion and intraparticle diffusion, both of which are relatively slower mechanisms. Consequently, while longer contact times improve adsorption in the shaker setup, the absence of ultrasound-induced turbulence results in a slower approach to equilibrium and slightly lower overall efficiency. The similar kinetic intensification effects of ultrasound have been reported for metal ion adsorption in previous studies, where ultrasonic energy enhanced diffusion rates and reduced equilibrium times [24,25,26]. These findings support the conclusion that ultrasound-assisted systems offer superior performance in terms of both the adsorption rate and overall efficiency compared with conventional agitation methods.

3.2.3. Effect of the dose of adsorbent

The effect of the dose of adsorbent on the efficiency of Ni(II) ions removal is demonstrated for both ultrasonic and shaker systems at the constant contact time of 60 min and pH value of 5, as shown in Figure ۵. In both systems, the efficiency increased sharply as the adsorbent mass rose from 2 g to 8 g due to the greater availability of active sites. Beyond 8–10 g, the improvement leveled off, likely because of particle aggregation and site overlap that reduced the effective surface area.

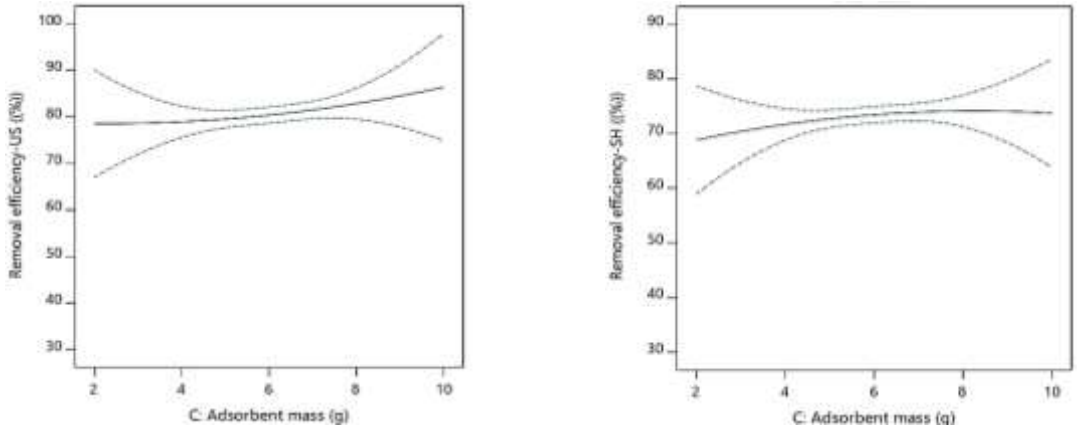

A) **B)**

Figure 5. Effect of the dose of adsorbent on the efficiency of Ni(II) removal, (A): ultrasonic system (B): shaker.

The ultrasonic system achieved higher performance (84.3 %) than the shaker (79.5 %) at 10 g and 60 min, owing to acoustic cavitation and microstreaming, which enhanced the dispersion of nanoparticle and accelerated mass transfer. In contrast, adsorption in the shaker system was limited by slower molecular diffusion. Similar results have been reported for the ultrasound-assisted adsorption of heavy metals, where ultrasound energy and increased surface area led to higher efficiencies and shorter equilibrium times [19,20,24,25,26]. These findings confirm that the dose of 8–10 g of the adsorbent offers an optimal balance between surface availability and particle dispersion.

3.2.4. Binary interaction

Three-dimensional response surface plots (Figure 6) were developed to illustrate the combined effects of pH, contact time, and adsorbent dosage on Ni(II) removal efficiency. The curved surfaces illustrate strong interactions among variables in both systems. In the ultrasonic setup, the efficiency increased by rising the pH and contact time up to an optimum region before leveling off.

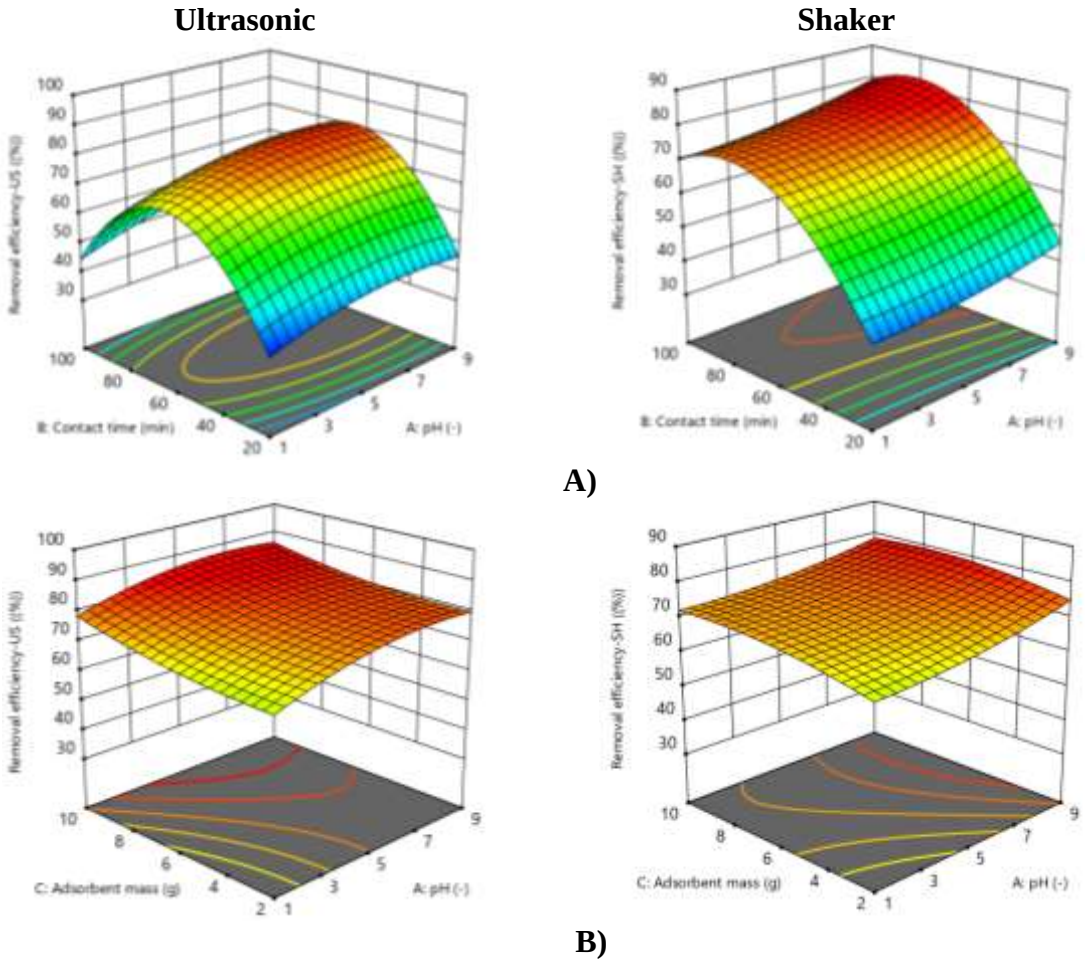

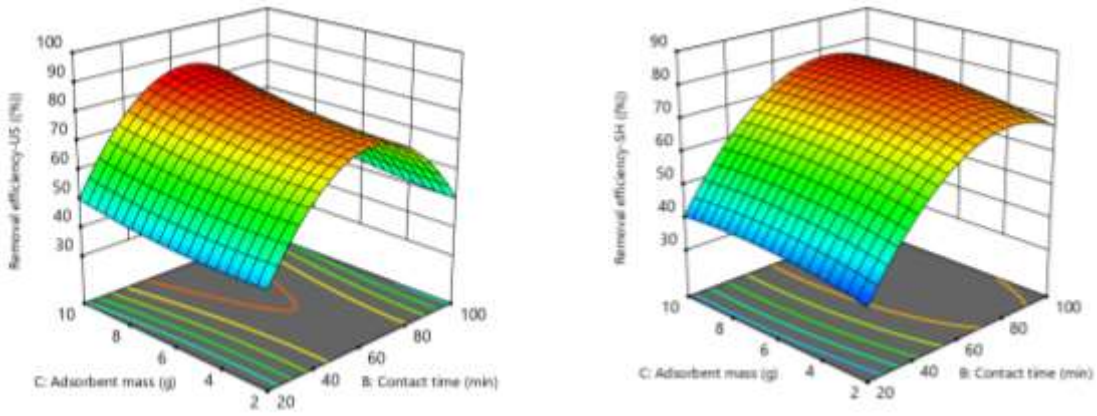

C)

Figure 6. Influence of the binary interaction of parameters on the efficiency of Ni(II) removal through 3D response surface, the (A) pH and contact time, (B) dose of adsorbent and pH, (C) dose of adsorbent and contact time.

3.3. Optimization

The adsorption process parameters were optimized using Response Surface Methodology (RSM) with a Central Composite Design (CCD). The aim was to determine the optimal combination of the pH, contact time, and adsorbent mass that maximizes the efficiency of Ni(II) removal under both ultrasonic and shaker conditions. The statistical optimization results revealed that the desirability function reached a value of 1.000, indicating that the developed models accurately predicted the maximum efficiency of Ni(II) removal. The optimal conditions were found at the pH = 8.1, contact time = 66 min, and dose of adsorbent = 8.6 g, resulting in a predicted removal efficiency of 84.8 % for the ultrasonic system and 80.0 % for the shaker system. These findings confirm that the ultrasound-assisted process provides higher efficiency under milder conditions and in shorter contact times. The improvement in the adsorption performance under ultrasonic conditions can be attributed to the enhanced mass transfer and boundary-layer disruption, which reduce film resistance and promote the faster diffusion of metal ions toward the active surface sites. The strong agreement between the predicted and experimental results validates the reliability of the RSM models and the adequacy of the optimization approach.

4. Conclusions

This study investigated the effect of the high-frequency ultrasonic irradiation on the adsorption of nickel (II) ions from aqueous solutions using Fe_3O_4 nanoparticles. The main findings can be summarized as follows:

1. Ultrasonic irradiation significantly enhanced the adsorption performance, achieving a maximum removal efficiency of 84.3% within 60 minutes at the pH = 5 and an adsorbent dosage of 8 g, compared to 79.54% obtained under the conventional stirring at 100 minutes and the pH = 9.
2. The pH and contact time were identified as the most influential factors affecting Ni(II) removal, as confirmed by the response surface methodology (RSM) and ANOVA analysis.
3. The application of ultrasound accelerated the adsorption process by generating cavitation and microstreaming, which improved mass transfer and prevented the agglomeration of nanoparticles.
4. The optimal operational conditions predicted by the RSM model (the pH = 8.1,

contact time = 66 min, and dose of adsorbent = 8.6 g) yielded a predicted efficiency of 84.8%, which was in close agreement with the experimental results.

Overall, the integration of ultrasonic irradiation with magnetic Fe_3O_4 nanoparticles presents a rapid, efficient, and eco-friendly method for removing heavy metal ions from wastewater. This hybrid technique can be extended to the treatment of other toxic metal pollutants, offering a sustainable alternative for the industrial effluent management.

References

[1] Buzea C, Pacheco Blandino II, Robbie K (2007) Nanomaterials and nanoparticles: Sources and toxicity. Biointerphases 2: 17–172. https://doi.org/10.1116/1.2815690

[2] Cao G (2004) Nanostructure & Nanomaterials: Synthesis, Properties & Applications. London: Imperial College Press.

[3] Wang R, Li BG, Huang T, Shi L (2007) $NbCl_5$-catalyzed one-pot Mannich-type reaction: Three-component synthesis of β-amino carbonyl compounds. Tetrahedron Letters 48: 2071–2073. https://doi.org/10.1016/j.tetlet.2007.01.142

[4] Yoichi M, Yamada A, Uozumi Y (2007) Development of a convoluted polymeric nanopalladium catalyst. Tetrahedron Letters 63: 8492–8498. https://doi.org/10.1016/j.tet.2007.05.071

[5] Jiang W, Zhou Y, Zhang Y, Xuan S, Gong X (2012) Superparamagnetic Ag@Fe_3O_4 core–shell nanospheres: Fabrication, characterization and application as reusable nanocatalysts. Dalton Transactions 41: 4594–4601. https://doi.org/10.1039/C2DT12307J

[6] Zhong CJ, Maye M (2001) Core–shell assembled nanoparticles as catalysts. Advanced Materials 13: 1507–1511. https://doi.org/10.1002/1521-4095(200110)13:19

[7] Hua M, Zhang S, Pan B, Zhang W, Zhang QX, Zhang LL (2012) Heavy metal removal from water by nanosized metal oxides: A review. Journal of Hazardous Materials 211: 317–331. https://doi.org/10.1016/j.jhazmat.2011.10.016

[8] Demiral H, Demiral I, Tumsek F, Karabacakoglu B (2008) Adsorption of chromium(VI) from aqueous solution by activated carbon derived from olive bagasse. Chemical Engineering Journal 138: 188–196. https://doi.org/10.1016/j.cej.2008.01.020

[9] Choi SUS (1995) Enhancing thermal conductivity of fluids with nanoparticles. ASME FED 231: 99–103.

[10] Rashin MN, Hemalatha J (2014) Magnetic and ultrasonic studies on stable cobalt ferrite magnetic nanofluid. Ultrasonics 54: 834–840. https://doi: 10.1016/j.ultras.2013.10.009

[11] Mahdavi M, Ahmad MB, Haron MJ, Namvar F, Nadi B, Rahman MZA (2013) Synthesis and characterization of biocompatible magnetic iron oxide nanoparticles. Molecules 18: 7533–7548. https://doi.org/10.3390/molecules18077533

[12] Yuanbi Z, Zumin Q, Huang J (2008) Fe_3O_4 magnetic nanoparticles as targeted drug carriers. Chinese Journal of Chemical Engineering 16: 451–455. https://doi.org/10.1016/S1004-9541(08)60104-4

[13] Chang YC, Chen DH (2005) Preparation and adsorption properties of chitosan-bound Fe_3O_4 nanoparticles for Cu(II) removal. Journal of Colloid and Interface Science 283: 446–451. https://doi.org/10.1016/j.jcis.2004.09.010

[14] Zhu GP, Nguyen NT (2012) Rapid magnetofluidic mixing in a uniform magnetic field. Lab on a Chip 12: 4772–4780. https://doi.org/10.1039/C2LC40818J

[15] Luque de Castro MD, Priego Capote F (2007) Analytical Applications of Ultrasound. 1st Ed. Elsevier, Spain.

[16] Thompson LH, Doraiswamy LK (2000) The rate-enhancing effect of ultrasound by inducing supersaturation in solid–liquid systems. Chemical Engineering Science 55: 3085–3090. https://doi.org/10.1016/S0009-2509(99)00481-9

[17] Lim M, Son Y, Khim J (2011) Frequency effects on the sonochemical degradation of chlorinated compounds. Ultrasonics Sonochemistry 18: 460–465. https://doi.org/10.1016/j.ultsonch.2010.07.021

[18] Fatehi MH, Shayegan J, Zabihi M, Goodarznia I (2017) Functionalized magnetic nanoparticles supported on activated carbon for adsorption of Pb(II) and Cr(VI) ions from saline solutions. Environmental Chemical Engineering 5: 1754–1762. https://ui.adsabs.harvard.edu/link_gateway/2017JEChE...5.1754F/doi:10.1016/j.jece.2017.03.006

[19] Franco DSP, Cunha JM, Dortzbacher GF, Dotto GL (2017) Adsorption of Co(II) from aqueous solutions onto rice husk modified by ultrasound-assisted and supercritical technologies. Process Safety and Environmental Protection 109: 55-62. https://doi.org/10.1016/j.psep.2017.03.029

[20] Zare-Dorabei R, Ferdowsi SM, Barzin A, Tadjarodi A (2016) Ultrasonic-assisted adsorption of Pb(II), Cd(II), Ni(II) and Cu(II) ions by graphene oxide modified with dipyridylamine. Ultrasonics Sonochemistry 32: 265-276. https://doi.org/10.1016/j.ultsonch.2016.03.020

[21] Mohammadi F, Rahimi M, Parvareh A, Feyzi M (2017) Stimulation of magnetic nanoparticles to intensify transesterification of soybean oil in micromixers for biodiesel production. Chemical Engineering and Processing: Process Intensification 122: 109–121. https://doi.org/10.1016/j.cep.2017.10.007

[22] Mohammadi F, Moradpour N, Azimi N, Ebrahimi E (2024) Feasibility of the purification of pharmaceuticals from aqueous solutions using carbon nanotubes in the presence of oxidizers. Iranian Journal of Chemical Engineering (IJChE) 21(2): 43-55. https://doi.org/10.22034/ijche.2024.443106.1523

[23] Mohammadi F, Jan Amiri R, Azimi N, Salimi F (2024) Achieving optimal conditions of membrane bioreactors for dairy industry wastewater treatment. Iranian Journal of Chemical Engineering (IJChE) 21(3): 49–65. https://doi.org/10.22034/ijche.2024.457926.1533

[24] Ghaedi M, Asfaram A, Hajati S, Goudarzi A, Bazrafshan AA (2015) Simultaneous ultrasound-assisted ternary adsorption of dyes onto copper-doped ZnS nanoparticles supported on activated carbon. Spectrochimica Acta Part A: Molecular and Biomolecular Spectroscopy 145: 203- 212. https://doi.org/10.1016/j.saa.2015.03.006

[25] Jing G, Zhou Z, Song L, Dong M (2011) Ultrasound-enhanced adsorption and desorption of chromium(VI) on activated carbon and polymeric resin. Desalination 279: 423–427. https://doi.org/10.1016/j.desal.2011.06.001

[26] Bao J, Fu Y, Bao Z (2013) Thiol-functionalized magnetite/graphene oxide hybrid as a reusable adsorbent for Hg(II) removal. Nanoscale Research Letters 8: 1–6. https://doi.org/10.1186/1556-276X-8-486